Phys., vol. 28, Apr. 1957, pp. 399–404.
[3] B. Lax and K. J. Button, *Microwave Ferrites and Ferrimagnetics*, 1st ed. New York: McGraw-Hill, 1962, p. 154.
[4] T. Kohane and E. Schlömann, "Linewidth and off-resonance loss in polycrystalline ferrites at microwave frequencies," *J. Appl. Phys.*, vol. 39, Feb. 1968, p. 720–721.
[5] C. E. Patton, "Effective linewidth due to porosity and anisotropy in polycrystalline yttrium iron garnet and Ca-V-substituted yttrium iron garnet at 10 GHz," *Phys. Rev.*, vol. 179, Mar. 1969, pp. 352–358.
[6] Q. H. F. Vrehen, "Absorption and dispersion in porous and anisotropic polycrystalline ferrites at microwave frequencies," *J. Appl. Phys.*, vol. 40, Mar. 1969, pp. 1849–1860.
[7] C. Borghese and R. Roveda, "Grain size average and distribution effects on the magnetic losses and threshold fields in nickel ferrites at microwave frequencies," *J. Appl. Phys.*, vol. 40, Nov. 1969, pp. 4791–4797.
[8] R. Roveda and C. Borghese, "Joint effect of fine grains and Co^{2+} relaxers on the high power and loss properties of Mg, Mn ferrites, at X-band," *J. Appl. Phys.*, vol. 41, May 1970, pp. 2729–2730.
[9] C. Borghese and R. Roveda, "Fine particles and fast relaxers influence on the magnetic RF threshold fields and losses in YIG," presented at Int. Conf. Magnetisme, Grenoble, France, Sept. 14–19, 1970; also to be published in *J. de Physique*.
[10] E. G. Spencer, L. A. Ault, and R. C. LeCraw, "Intrinsic tensor permeabilities on ferrite rods, spheres, and disks," *Proc. IRE*, vol. 44, pp. 1311–1317, Oct. 1956.
[11] E. Schlömann, "Properties of magnetic materials with a non-uniform saturation magnetization. II: Longitudinal susceptibility," *J. Appl. Phys.*, vol. 38, pp. 5035–5044, Dec. 1967; also T. Kohane and E. Schlömann," Longitudinal susceptibility of porous polycrystalline YIG at microwave frequencies," *J. Appl. Phys.*, vol. 37, Mar. 1966, pp. 1073–1074.
[12] R. I. Joseph and E. Schlömann, "Transient and steady-state absorption of microwave power under parallel pumping theory," *J. Appl. Phys.*, vol. 38, Mar. 1967, pp. 1915–1928.
[13] W. E. Case, R. D. Harrington, and L. B. Schmidt, "Ferromagnetic resonance in polycrystalline ferrite and garnet disks at L-band frequencies," *J. Res. Nat. Bur. Stand.*, vol. 68C, Apr.–June 1964, pp. 85–91.
[14] Q. H. F. Vrehen, H. G. Beljers, and J. G. M. De Lau, "Microwave properties of fine grain Ni and Mg ferrites," *IEEE Trans. Magn.*, vol. MAG-5, Sept. 1969, pp. 617–621.
[15] R. Roveda and G. Cattarin, "Circolatori a giunzione ad Y in guida d'onda per alte potenze medie e di picco per impieghi radaristici," *Rendiconti Annuali AEI*, 1970.
[16] D. Polder and J. Smit, "Resonance phenomena in ferrites," *Rev. Mod. Phys.*, vol. 25, Oct. 1953, pp. 89–90.
[17] C. E. Fay and R. L. Comstock, "Operation of the ferrite junction circulator," *IEEE Trans. Microwave Theory Tech.*, vol. MTT-13, Jan. 1965, pp. 15–27.

Analytical and Numerical Studies of the Relative Convergence Phenomenon Arising in the Solution of an Integral Equation by the Moment Method

RAJ MITTRA, FELLOW, IEEE, TATSUO ITOH, MEMBER, IEEE, AND TI-SHU LI, STUDENT MEMBER, IEEE

Abstract—**The relative convergence phenomenon that occurs in the numerical solution of the integral equation for the iris discontinuity problem is studied both analytically and numerically. It is shown that the solution for the aperture field can be highly dependent upon the manner in which the kernel and the unknown function are approximated in the process of constructing a matrix equation by the moment method. An analytical explanation is provided for the above phenomenon and the theoretical predictions are verified numerically. Also included is a suggested numerical algorithm for detecting and alleviating the relative convergence behavior for more general problems.**

I. Introduction

IT WAS pointed out a number of years ago [1] that the manner in which one partitions a doubly infinite matrix arising in the formulation of the boundary value problem in a bifurcated waveguide significantly affects the results for the scattering coefficients in the guide. This phenomenon was referred to as "relative convergence" and it was proven that there exists a unique choice for the partitioning ratio that yields the correct result. It was also demonstrated that anything but the correct choice of partitioning will lead to results that violate the "edge condition" [2].

Recently it was discovered that the relative convergence phenomenon also occurs in a variety of other problems [3]–[5], even where a completely different mode of formulation is employed. It was found, for instance, that the matrix equation obtained by the mode matching formulation [6], [7] or by the application of the moment method to integral equations exhibits relative convergence. As an example, it has been found that the integral equation

$$\int_0^b K(x, x')\psi(x')dx' = g(x), \qquad 0 < x < b \qquad (1)$$

for the iris discontinuity problem in a waveguide ex-

Manuscript received December 10, 1970; revised March 24, 1971. This work was supported by U. S. Army Research Grant DA-ARO-G1103. The major portion of this paper was presented at the Fall URSI Meeting, Columbus, Ohio, September 1970.

The authors are with the Antenna Laboratory, Department of Electrical Engineering, University of Illinois, Urbana, Ill. 61801.

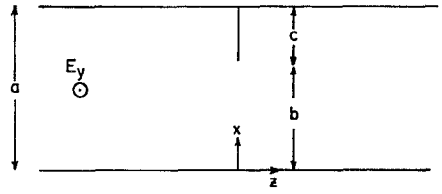

Fig. 1. Inductive iris in parallel-plate waveguide.

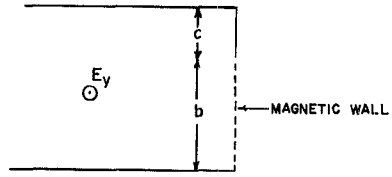

Fig. 2. Equivalent geometry of inductive iris in case of symmetrical excitation.

hibits a relative convergence phenomenon when solved by the moment method. That is, if $\psi(x)$, the unknown, is approximated in terms of an M-term Fourier series

$$\psi(x) = \sum_{m=1}^{M} B_m \phi_m(x) \tag{2}$$

then the best approximation to the true solution is obtained for a critical value of M, say M_c. The critical value M_c is in turn dependent on P, the number of terms retained in the truncated form of series representation for the kernel

$$K(x, x') = \sum_{n=1}^{P} \alpha_n \chi_n(x) \chi_n(x'). \tag{3}$$

For the iris problem, the χ_n's are the Fourier series basis functions for the range $0 < x < a$, and a is the transverse dimension of the waveguide.

The purpose of this paper is twofold: to provide an analytical explanation of the relative convergence phenomenon arising in the iris discontinuity problem; and to suggest a numerical approach for detecting and resolving the relative convergence phenomenon.

In Section II, an integral equation is derived for the iris discontinuity in the waveguide and transformed into a matrix equation using the moment method. An alternative set of equations is derived for the same problem in Section III, using the mode matching method. This set of alternative equations, although equivalent to those derived earlier by the moment method, are found to be more convenient for analytical processing.

In Section IV, the modified residue calculus technique is applied to solve the matrix equation obtained by the mode matching method. The critical value of M is now determined by investigating the asymptotic behavior of a generating function of complex variable, the residues of which are related to the unknown modal coefficients in the waveguide.

Finally, some numerical results that support the theoretical predictions of Section IV are presented in Section V. A method for detecting the relative convergence phenomenon and extracting the correct solution in the presence of this phenomenon is suggested on the basis of the numerical experiments on the iris problem.

II. Moment Method of Solution

The geometry for the iris discontinuity problem in the parallel-plate waveguide is shown in Fig. 1. The discussion below will be restricted to the TE case only, although the analysis for the TM case can be carried out along similar lines. It is well known that the solution to the original iris problem can be derived from those of two auxiliary problems—the symmetrical and asymmetrical excitations. For the latter case, the aperture ($z = 0$, $0 < x < b$) is replaced by the electric wall, and hence, the problem becomes a trivial one. The symmetrical case leads to the auxiliary problem shown in Fig. 2, where the aperture is replaced by a magnetic wall. In the following, only this auxiliary problem is treated since it contains the necessary information for constructing the solution to the original problem.

The first step is to write the total field in terms of the eigenfunctions of the waveguide when the TE_{s0} mode is incident from the left.

$$E_y(x, z) = \sin\frac{s\pi x}{a} e^{-\alpha_s z} + \sum_{n=1}^{\infty} A_n \sin\frac{n\pi x}{a} e^{+\alpha_n z} \tag{4}$$

$$\alpha_n = \left[\left(\frac{n\pi}{a}\right)^2 - k^2\right]^{1/2} = j\left[k^2 - \left(\frac{n\pi}{a}\right)^2\right]^{1/2}. \tag{5}$$

All the other field components are derivable from this expression. In view of the boundary conditions at the plane $z = 0$, we have

$$E_y(x, 0) = \sin\frac{s\pi x}{a} + \sum_{n=1}^{\infty} A_n \sin\frac{n\pi x}{a} = \begin{cases} \psi(x), & 0 < x < b \\ 0, & b < x < a \end{cases} \tag{6}$$

$$\frac{\partial E_y}{\partial z}(x, 0) = -\alpha_s \sin\frac{s\pi x}{a} + \sum_{n=1}^{\infty} \alpha_n A_n \sin\frac{n\pi x}{a} = \begin{cases} 0, & 0 < x < b \\ \xi(x), & b < x < a \end{cases} \tag{7}$$

where $\psi(x)$ is unknown aperture E field for $0 < x < b$, and $\xi(x)$ is proportional to the unknown surface current on the slit, $b < x < a$.

By Fourier analyzing (6) and substituting A_n into (7), we may derive the integral equation for the aperture field $\psi(x)$:

$$\int_0^b K(x, x')\psi(x')dx' = g(x), \qquad 0 < x < b \tag{8}$$

where

$$K(x, x') = \sum_{n=1}^{\infty} \alpha_n \sin\frac{n\pi x}{a} \sin\frac{n\pi x'}{a} \tag{9}$$

is the kernel and

$$g(x) = a\alpha_s \sin\frac{s\pi x}{a} \tag{10}$$

the known inhomogeneous term.

To solve the integral equation (8) by one of the moment methods, say Galerkin's method [8], we first approximate $\psi(x)$ with a finite number of basis functions

$$\psi(x) = \sum_{m=1}^{M} B_m \phi_m(x), \qquad \phi_m(x) = \sin\frac{m\pi x}{b}. \tag{11}$$

Next, we substitute (11) into (8) and take the inner product of (8) with the weight functions $\phi_l(x)$, $l=1, 2, \cdots, M$. The result is the $M\times M$ matrix equation.

$$\sum_{m=1}^{M} B_m <\phi_l, \tilde{K}\phi_m> = <\phi_l, g>, \qquad l = 1, 2, \cdots, M \tag{12}$$

where $\tilde{K}$ is an integral operator given by

$$\tilde{K} = \int_0^b dx' K(x, x') \tag{13}$$

and the inner product $<\phi_l, g>$ is explicitly written as

$$<\phi_l, g> = \int_0^b \phi_l(x) g(x) dx. \tag{14}$$

The exact solution to the integral equation can in principle be obtained from (12) after letting $M\to\infty$. In practice, however, M is necessarily finite and the summation in $K(x, x')$ must also be truncated, say at $n=P$.

After carrying out the necessary integrations, (12) can be explicitly written as

$$\sum_{m=1}^{M} B_m \left[(-1)^m \frac{m\pi}{b} \sum_{n=1}^{P} \frac{\alpha_n \sin^2\frac{n\pi b}{a}}{(\alpha_n^2 - \beta_l^2)(\alpha_n^2 - \beta_m^2)} \right] = a\alpha_s \frac{\sin\frac{s\pi b}{a}}{\alpha_s^2 - \beta_l^2}, \qquad l = 1, 2, \cdots, M \tag{15}$$

where

$$\beta_m = \left[\left(\frac{m\pi}{b}\right)^2 - k^2\right]^{1/2} = j\left[k^2 - \left(\frac{m\pi}{b}\right)^2\right]^{1/2}. \tag{16}$$

III. Mode Matching Method of Solution

In Section II we transformed the integral equation into a matrix equation using the moment method. In this section an alternative set of equations is derived by an application of the mode matching method.

First, we introduce an auxiliary geometry shown in Fig. 3, where a small septum of length δ is introduced. It is evident that the original structure in Fig. 2 can be recovered by letting $\delta\to 0$ in the auxiliary geometry. We now write the eigenfunction expansions for the fields in

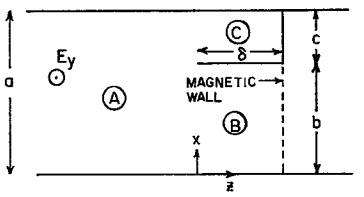

Fig. 3. Auxiliary geometry for iris discontinuity problem.

the fictitious waveguides B and C as follows:

$$E_y(x, z) = \sum_{n=1}^{M} B_n \sin\frac{n\pi x}{b} \left\{e^{-\beta_n z} + e^{\beta_n (z-\delta)}\right\}/2, \qquad 0 < x < b \tag{17}$$

$$E_y(x, z) = \sum_{n=1}^{N} C_n \sin\frac{n\pi(a-x)}{c} \left\{e^{-\gamma_n z} - e^{\gamma_n (z-\delta)}\right\}/2, \qquad b < x < a \tag{18}$$

where β_n is given by (16) and

$$\gamma_n = \left[\left(\frac{n\pi}{c}\right)^2 - k^2\right]^{1/2} = j\left[k^2 - \left(\frac{n\pi}{c}\right)^2\right]^{1/2}. \tag{19}$$

Note that the infinite summations in (17) and (18) are truncated at M and N, respectively. After truncating the summation in (4) at $n=P$, we match the fields at the interface $z=0$. Letting δ go to zero, we obtain the equations

$$\sin\frac{s\pi x}{a} + \sum_{n=1}^{P} A_n \sin\frac{n\pi x}{a} = \sum_{n=1}^{M} B_n \sin\frac{n\pi x}{b}, \qquad 0 < x < b \tag{20a}$$

$$-\alpha_s \sin\frac{s\pi x}{a} + \sum_{n=1}^{P} \alpha_n A_n \sin\frac{n\pi x}{a} = 0, \qquad 0 < x < b \tag{20b}$$

$$\sin\frac{s\pi x}{a} + \sum_{n=1}^{P} A_n \sin\frac{n\pi x}{a} = 0, \qquad b < x < a \tag{21a}$$

$$-\alpha_s \sin\frac{s\pi x}{a} + \sum_{n=1}^{P} \alpha_n A_n \sin\frac{n\pi x}{a} = -\sum_{n=1}^{N} \gamma_n C_n \sin\frac{n\pi(a-x)}{c}, \qquad b < x < a. \tag{21b}$$

The next step is to transform these equations into the spectral domain by eliminating the x variation. To this end we multiply (20) by $\sin(m\pi x/b)$ and integrate from 0 to b. Also, (21) is multiplied by $\sin\{m\pi(a-x)/c\}$ and integrated from b to a. This gives

$$\frac{\sin\frac{s\pi b}{a}}{\alpha_s^2 - \beta_m^2} + \sum_{n=1}^{P} \frac{\bar{A}_n}{\alpha_n^2 - \beta_m^2} = (-1)^m \frac{b^2}{2m\pi} B_m, \qquad m = 1, 2, \cdots, M \tag{22a}$$

$$-\frac{\alpha_s \sin\frac{s\pi b}{a}}{\alpha_s^2 - \beta_m^2} + \sum_{n=1}^{P} \frac{\alpha_n \bar{A}_n}{\alpha_n^2 - \beta_m^2} = 0, \qquad m = 1, 2, \cdots, M \tag{22b}$$

$$\frac{\sin\frac{s\pi b}{a}}{\alpha_s^2-\gamma_m^2}+\sum_{n=1}^{P}\frac{\overline{A}_n}{\alpha_n^2-\beta_m^2}=0,$$

$$m=1,2,\cdots,N \quad (23a)$$

$$-\frac{\alpha_s\sin\frac{s\pi b}{a}}{\alpha_s^2-\gamma_m^2}+\sum_{n=1}^{P}\frac{\alpha_n\overline{A}_n}{\alpha_n^2-\gamma_m^2}=(-1)^{m+1}\frac{c^2}{2m\pi}C_m,$$

$$m=1,2,\cdots,N \quad (23b)$$

where

$$\overline{A}_n=A_n\sin\frac{n\pi b}{a}. \quad (24)$$

By choosing $M+N=P$, we can solve the $P\times P$ matrix equation comprising (22b) and (23a). Substituting the resulting $\overline{A}_n$'s into (22a) we may then obtain the expansion coefficients B_m of the aperture E field in the region $0<x<b$.

We may also derive an alternative set of equations by Fourier analyzing (20) and (21) in the range $0<x<a$. The equations read

$$\frac{a}{2}[\delta_s{}^m+A_m]=\sin\frac{m\pi b}{a}\sum_{n=1}^{M}\frac{(-1)^{n+1}\frac{n\pi}{b}B_n}{\beta_n^2-\alpha_m^2},$$

$$m=1,2,\cdots,P \quad (25a)$$

$$\frac{a}{2}\alpha_m[\delta_s{}^m-A_m]=\sin\frac{m\pi b}{a}\sum_{n=1}^{N}\frac{(-1)^{n+1}\frac{n\pi}{c}\gamma_nC_n}{\gamma_n^2-\alpha_m^2},$$

$$m=1,2,\cdots,P. \quad (25b)$$

The above set of equations allow us to solve for B_n and C_n directly by choosing $M+N=P$ and eliminating A_m.

Our next step is to show the equivalence between the moment method and the mode matching method. To this end, we eliminate A_n from (22b) and (25a) and obtain

$$\sum_{m=1}^{M}B_m\left[\sum_{n=1}^{P}\alpha_n\frac{(-1)^m\frac{m\pi}{b}\sin^2\frac{n\pi b}{a}}{(\alpha_n^2-\beta_m^2)(\alpha_n^2-\beta_l^2)}\right]=a\alpha_s\frac{\sin\frac{s\pi b}{a}}{\alpha_s^2-\beta_l^2}. \quad (26)$$

We observe that (26) is identical to (15) obtained earlier by the moment method. Having demonstrated the equivalence between the truncated forms of matrix equation derived via mode matching and moment methods, we return to (22) and (23) and construct an analytical representation for its solution. The reason for our going through this elaborate procedure of deriving the auxiliary equations and showing their equivalence to (15) is that the latter set does not lend itself directly to convenient analytical processing.

IV. Investigation by the Modified Residue Calculus Technique

The modified residue calculus technique [9], [10] is a useful method for solving the infinite set of equations of the type (22) and (23). The method has a number of unique features, one of which is its ability to enforce the satisfaction of the edge condition. We will make use of this feature to investigate the relative convergence phenomena.

To this end, we first multiply (22a) and (23a) by β_m and γ_m, respectively, and add and subtract the resulting equations from (22b) and (23b). We then obtain

$$-\frac{\sin\frac{s\pi b}{a}}{\alpha_s+\beta_m}+\sum_{n=1}^{P}\frac{\overline{A}_n}{\alpha_n-\beta_m}=(-1)^m\frac{b^2\beta_m}{2m\pi}B_m,$$

$$m=1,2,\cdots,M \quad (27a)$$

$$-\frac{\sin\frac{s\pi b}{a}}{\alpha_s-\beta_m}+\sum_{n=1}^{P}\frac{A_n}{\alpha_n+\beta_m}=(-1)^{m+1}\frac{b^2\beta_m}{2m\pi}B_m,$$

$$m=1,2,\cdots,M \quad (27b)$$

$$-\frac{\sin\frac{s\pi b}{a}}{\alpha_s+\gamma_m}+\sum_{n=1}^{P}\frac{\overline{A}_n}{\alpha_n-\gamma_m}=(-1)^{m+1}\frac{c^2\gamma_m}{2m\pi}C_m,$$

$$m=1,2,\cdots,N \quad (28a)$$

$$-\frac{\sin\frac{s\pi b}{a}}{\alpha_s-\gamma_m}+\sum_{n=1}^{P}\frac{\overline{A}_n}{\alpha_n+\gamma_m}=(-1)^{m+1}\frac{c^2\gamma_m}{2m\pi}C_m,$$

$$m=1,2,\cdots,N. \quad (28b)$$

Also eliminating B_m and C_m, we get

$$\sum_{n=1}^{P}\left(\frac{\overline{A}_n}{\alpha_n-\beta_m}+\frac{\overline{A}_n}{\alpha_n+\beta_m}\right)=\left(\frac{1}{\alpha_s+\beta_m}+\frac{1}{\alpha_s-\beta_m}\right)\sin\frac{s\pi b}{a},$$

$$m=1,2,\cdots,M \quad (29a)$$

$$\sum_{n=1}^{P}\left(\frac{\overline{A}_n}{\alpha_n-\gamma_m}-\frac{\overline{A}_n}{\alpha_n+\gamma_m}\right)=\left(\frac{1}{\alpha_s+\gamma_m}-\frac{1}{\alpha_s-\gamma_m}\right)\sin\frac{s\pi b}{a},$$

$$m=1,2,\cdots,N. \quad (29b)$$

The essential step in the modified residue calculus technique is the construction of a meromorphic func-

tion $f(\omega)$ satisfying the following conditions:

1) $f(\omega)$ has simple poles at $\omega=\alpha_n$, $n=1, 2, \cdots, P$, and at $\omega=-\alpha_s$.

2) $f(\beta_m)+f(-\beta_m)=0, \quad m=1, 2, \cdots, M, \quad M+N=P.$
$f(\gamma_m)-f(-\gamma_m)=0, \quad m=1, 2, \cdots, N, \quad M+N=P.$

3) $f(\omega)\sim\omega^{-\nu}, \quad 1<\nu<2$ as $|\omega| \to \infty$.

4) $R_f(-\alpha_s)=\sin\dfrac{s\pi b}{a}$

where $R_f(-\alpha_s)$ is the residue of $f(\omega)$ at $\omega=-\alpha_s$.

It is possible to relate the unknown coefficients A_n, B_n, etc., to the function $f(\omega)$ via the following manipulations. Consider the integrals appearing below with contours C as circles at infinity.

$$\frac{1}{2\pi j}\oint_C \left\{\frac{f(\omega)}{\omega-\beta_m}+\frac{f(\omega)}{\omega+\beta_m}\right\} d\omega$$

$$\frac{1}{2\pi j}\oint_C \left\{\frac{f(\omega)}{\omega-\gamma_m}-\frac{f(\omega)}{\omega+\gamma_m}\right\} d\omega.$$

Then it can be shown [9] that

$$A_n = R_f(\alpha_n), \qquad n = 1, 2, \cdots, P \tag{30}$$

$$B_m = (-1)^m\frac{2m\pi}{b^2\beta_m}f(-\beta_m), \qquad m = 1, 2, \cdots, M \tag{31}$$

$$C_m = (-1)^m\frac{2m\pi}{c^2\gamma_m}f(-\gamma_m), \qquad m = 1, 2, \cdots, N = P - M. \tag{32}$$

From these equations we see that once the function $f(\omega)$ is constructed, the problem can be considered as solved. A suitable form of $f(\omega)$ is

$$f(\omega) = Kg(\omega)p(\omega) \tag{33}$$

$$g(\omega) = \exp\left[\frac{1}{\pi}\left(b\ln\frac{a}{b}+c\ln\frac{a}{c}\right)\right]\frac{\pi(\omega,\beta)\pi(\omega,\gamma)}{(\omega+\alpha_s)\pi(\omega,\alpha)} \tag{34}$$

$$p(\omega) = 1+\sum_{p=1}^{M}\frac{\omega c_p}{\beta_p-\omega}+\sum_{q=1}^{M}\frac{\omega d_q}{\gamma_q-\omega} \tag{35}$$

where

$$\pi(\omega,\beta) = \prod_{n=1}^{M}\left(1-\frac{\omega}{\beta_n}\right)\exp\left(\frac{\omega b}{n\pi}\right) \tag{36a}$$

$$\pi(\omega,\gamma) = \prod_{n=1}^{N}\left(1-\frac{\omega}{\gamma_n}\right)\exp\left(\frac{\omega c}{n\pi}\right) \tag{36b}$$

$$\pi(\omega,\alpha) = \prod_{n=1}^{P}\left(1-\frac{\omega}{\alpha_n}\right)\exp\left(\frac{\omega a}{n\pi}\right). \tag{36c}$$

The unknown constants c_p and d_q are to be determined so that the condition 2) is satisfied, and the normalization constant K is determined from the condition 4). It should be remarked that except for a normalization constant, $g(\omega)$ can be identified with the exact solution for the semi-infinite bifurcation problem, i.e., the one where δ is infinite in Fig. 3.

We will not attempt to construct an exact form of $f(\omega)$ by determining c_p and d_q. Instead, we will merely investigate the asymptotic behavior of $f(\omega)$ when M, N, and P become large and show that only one critical choice of M/N gives the correct asymptotic behavior of $f(\omega)$, which, in turn, determines the behavior of the field coefficients A_n, B_n, and C_n for large n.

Note first that all of these coefficients must behave as

$$A_n,\ B_n,\ C_n \sim n^{-3/2}, \qquad \text{with } n \to \infty.$$

This is required by the physical constraint that the field must satisfy the edge condition [2]. From (30), (31), and (32), it can be shown that $\nu=3/2$ in the condition 3).

Mittra [1] proved that the canonical function $g(\omega)$ shows the relative convergence phenomena. That is, when $M, N, P\to\infty$,

$$g(\omega) \sim \omega^{-3/2}, \qquad |\omega| \to \infty \tag{37}$$

only if $M/N=b/c$, and $g(\omega)$ either decays or grows exponentially for any other choice of M/N. What we will now show is that, for an incorrect choice of the ratio M/N, the asymptotic behavior of $f(\omega)$ is the same as that of $g(\omega)$. This is because the perturbation factor $p(\omega)$ in $f(\omega)$ cannot alter the exponential behavior due to $g(\omega)$.

In the following, we consider the behavior of $p(\omega)$ as $|\omega|\to\infty$ for two different cases. It should be pointed out that for convergence reasons we need only consider the cases where c_p (or d_q) either decays exponentially or has the behavior p^μ, $\mu<0$.

Case 1

c_p decays exponentially

$$s(\omega) = \sum_{p=1}^{\infty}\frac{c_p}{\beta_p-\omega}\sim 0(\omega^{-1}) \tag{38}$$

and hence $p(\omega)\sim 0(\omega^0)$.

Case 2a

$$c_p \sim 0(p^\nu), \qquad -1<\nu<0.$$

We apply the Euler–Maclaurin sum formula [11]

$$s(\omega) \simeq \sum_{p=1}^{K-1}\frac{c_p}{\beta_p-\omega}+\sum_{p=K}^{\infty}\frac{c_0 p^\nu}{\frac{p\pi}{b}-\omega} \tag{39}$$

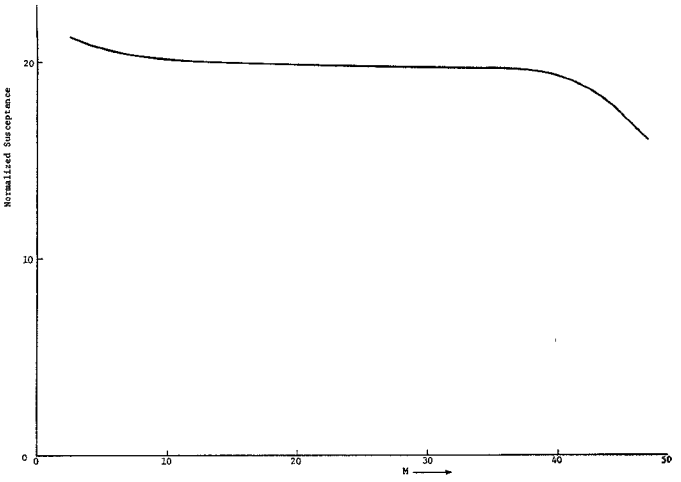

Fig. 4. Normalized susceptance of inductive iris versus values of M. TE_{10} incident, $b=0.4a$, $P=100$.

$$s(\omega) \simeq \sum_{p=1}^{K-1} \frac{c_p}{\beta_p - \omega} + \frac{c_0 b}{\pi} \left\{ \int_K^\infty h(x)dx + \frac{h(K)}{2} - \sum_{n=1}^{\infty} \frac{B_{2n}}{(2n)!} \frac{d^{(2n-1)}}{dx^{(2n-1)}} h(K) \right\} \quad (40)$$

where K is some large integer beyond which we can approximate $c_p \simeq c_0 p^\nu$ and $\beta_p \simeq p\pi/b$; B_{2n} are the Bernoulli numbers; and $h(x)$ is given by

$$h(x) = \frac{x^\nu}{p - \alpha}, \qquad \alpha = \frac{b\omega}{\pi}. \quad (41)$$

Using the Stieltjes transform [12] when $\arg \alpha \neq 0$ or the Hilbert transform [12] when $\arg \alpha = 0$, we find

$$\int_K^\infty h(x)dx = \int_0^K h(x)dx + K_0 \alpha^\nu \simeq 0(\alpha^\nu). \quad (42)$$

Hence

$$s(\omega) \sim 0(\omega^\nu), \qquad -1 < \nu < 0 \quad (43)$$

for large ω. This gives

$$p(\omega) \sim 0(\omega^{1+\nu}).$$

Case 2b

$c_p \sim 0(p^{-1})$

$$s(\omega) \simeq \sum_{p=1}^{\infty} \frac{c_0 \frac{b}{\pi}}{p(p - \alpha)} = \frac{c_0 b}{-\pi\alpha} \left\{ C_e - \frac{1}{\alpha} + \psi(-\alpha) \right\} \quad (44)$$

where C_e is the Euler's constant and $\psi(x)$ is the digamma function defined by

$$\psi(x) = \frac{d}{dx} \ln \Gamma(x). \quad (45)$$

$\Gamma(x)$ is the conventional gamma function and $\alpha = b\omega/\pi$.

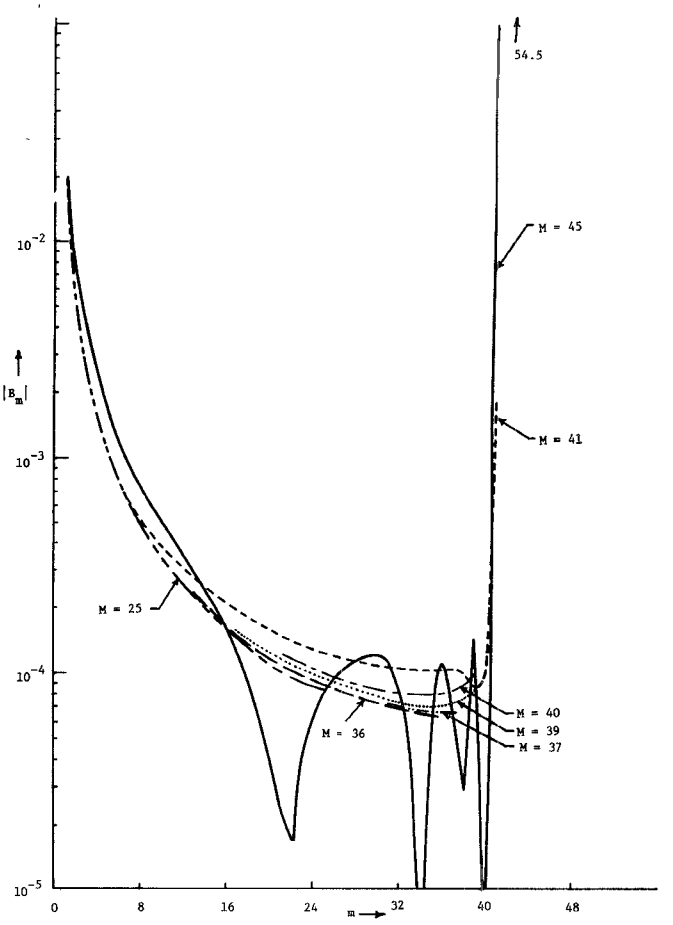

Fig. 5. Magnitude of B_m for inductive iris versus m. TE_{10} incident, $b=0.4a$.

The asymptotic form of $\psi(x)$ is

$$\psi(x) \sim \begin{cases} \ln x - \frac{1}{2x}, & |\arg x| < \pi \\ \ln(-x) - \pi \cot \pi x - \frac{1}{2x}, & \arg x = \pi. \end{cases} \quad (46)$$

Hence for large ω

$$\omega s(\omega) \sim 0(\ln \omega) \quad (47)$$

and

$$p(\omega) \sim 0(\ln \omega).$$

Case 2c

$$c_p \sim 0(p^\nu), \qquad \nu < -1.$$

It is easy to show that the summation converges uniformly and

$$s(\omega) \sim 0(\omega^{-1}) \quad (48)$$

and hence $p(\omega) \sim 0(\omega^0)$.

On the basis of the above results, we conclude that the presence of the factor $p(\omega)$ in $f(\omega)$ cannot alter its

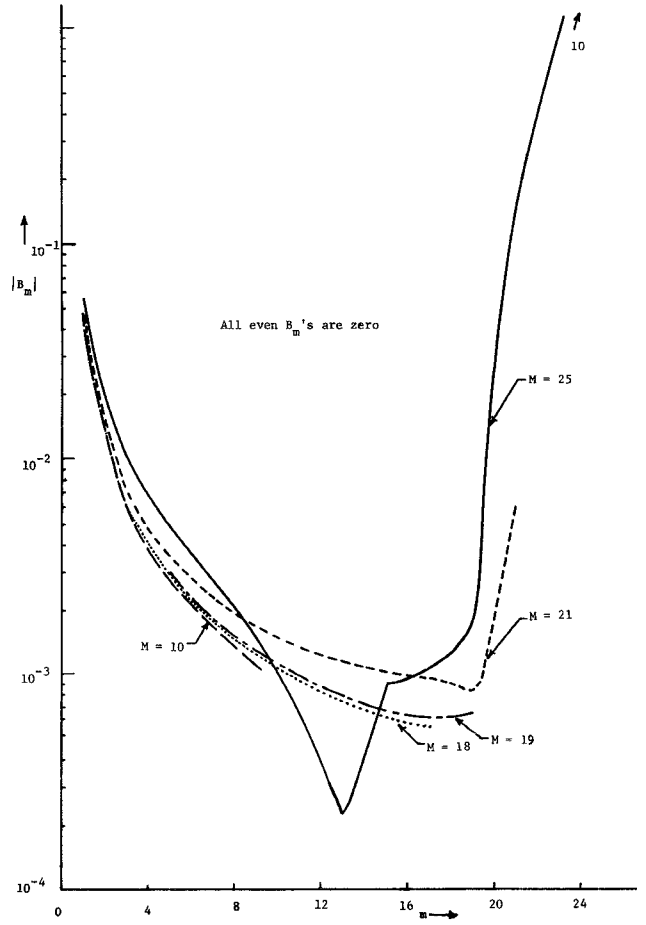

Fig. 6. Magnitude of B_m for symmetric inductive iris versus m. TE_{10} incident, 40 percent aperture width, $P=100$.

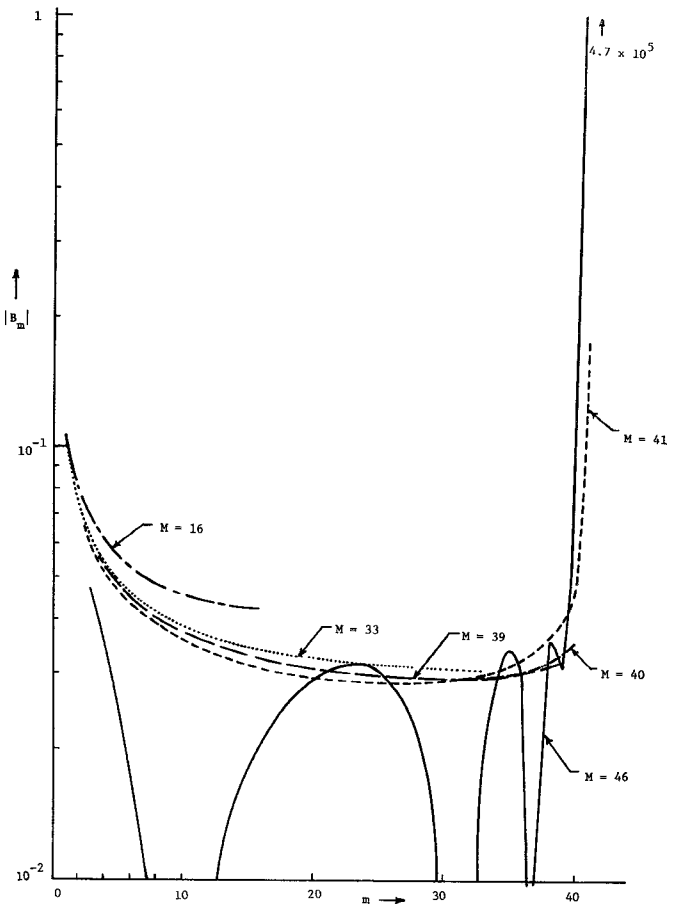

Fig. 7. Magnitude of B_m for capacitive iris versus m. TEM incident, $b=0.4a$, $P=100$.

asymptotic behavior when $g(\omega)$ either exponentially decays or grows for large ω. Hence, just as in the case of bifurcated waveguide, correct results are obtained only for the numerical choice of the ratio

$$M/P = b/a. \tag{49}$$

By reference to (30), (31), and (32), we note that the field coefficients have an exponential behavior for large n unless (49) is satisfied.

In addition to the theoretical explanation given above, it is possible to provide an intuitive interpretation[1] of the relative convergence phenomenon arising in the moment method of solution. Since the kernel $K(x, x')$ has been approximated by truncating the right-hand side of (3), the computations are insensitive to spatial oscillations of $\psi(x)$ that are more rapid than a certain fixed amount, which depends directly on P. Erroneous results must be obtained if M is so large that excessive spatial oscillations of $\psi(x)$ are included. The point is that if M is too large compared with P, then the matrix that has to be inverted becomes ill conditioned.

[1] The authors are grateful to one of the reviewers for suggesting this explanation.

V. Numerical Results and Discussion

In this section we present some numerical results in support of the predictions based upon the theoretical discussion in the last section. Fig. 4 shows the normalized susceptance of the inductive iris discontinuity. Because the ratio of the aperture area to the total guide dimension is 40 percent and $P=100$, then $M=40$ should give the best answer. It may be noticed that for $M<40$ the numerical value of susceptance is not greatly in error. However, for $M>40$ the numerical values for the susceptance deviate rather rapidly from the correct results.

We also note that on the basis of the susceptance calculations alone, it is not possible to select the correct value of M without resorting to experimental verification of the calculated data. We find, however, that the asymptotic behavior of the higher order coefficients B_m provides a reliable indication of the relative convergence phenomenon and at the same time serves as a guide for the correct choice of M. We can see by reference to Fig. 5 that the envelope of the higher order coefficients B_m decreases steadily with increasing m, providing that M is less than the critical value of 40.

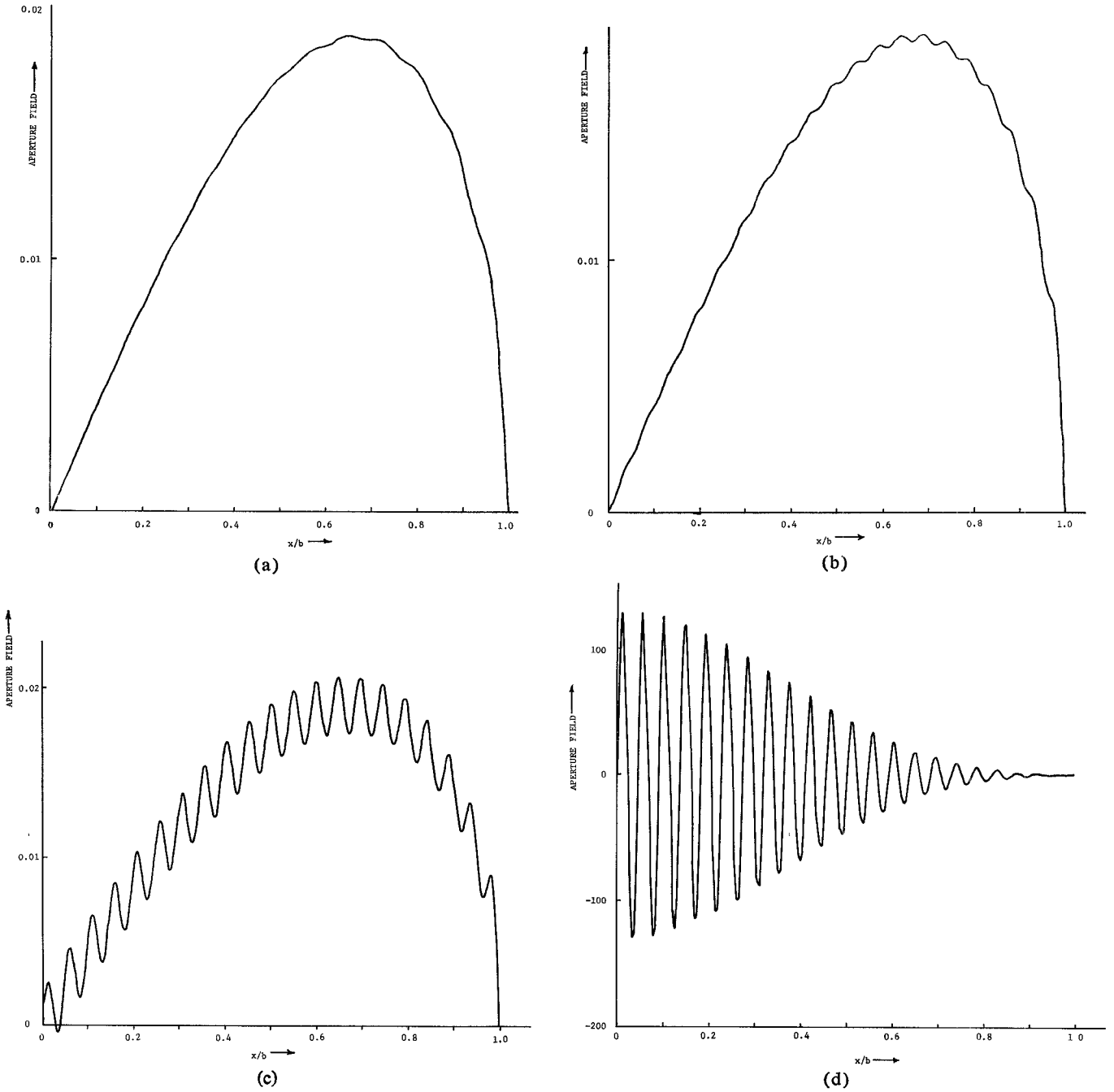

Fig. 8. Aperture E_y field for inductive iris. $b=0.4a$, $P=100$. (a) $M=25$. (b) $M=40$. (c) $M=41$. (d) $M=45$.

For values of M greater than the critical value of 40, the coefficients B_m exhibit an exponential growth for M larger than the critical value of $M=40$.

It can also be seen that B_m's exhibit a slight growth for large m for $M=39$; however, it is conjectured that this is due to numerical errors such as roundoff, truncation, etc.

Fig. 6 shows a similar behavior for the mode coefficients for the symmetric inductive iris. Because of symmetry, all of the even B_m's are zero in this case. Fig. 7 corresponds to the case of a capacitive iris discontinuity with a TEM mode incident. Once again the behavior of the modal coefficients above and below the critical choice of M is similar to the ones in Fig. 5.

Fig. 8 shows the aperture E_y field for TE_{10} incidence on the inductive iris. The aperture field was calculated using (11) after the B_m's had been computed. It is clear that up to $M=40$, the field-distribution plots exhibit little change with M, due primarily to the dominance of the lower order B_m coefficients. However, for $M>40$, the exponential growth of B_m's for $m>40$ causes the field distribution to be highly oscillatory, indicating a large error in the field computation. It is interesting to test whether the singular behavior prescribed by the

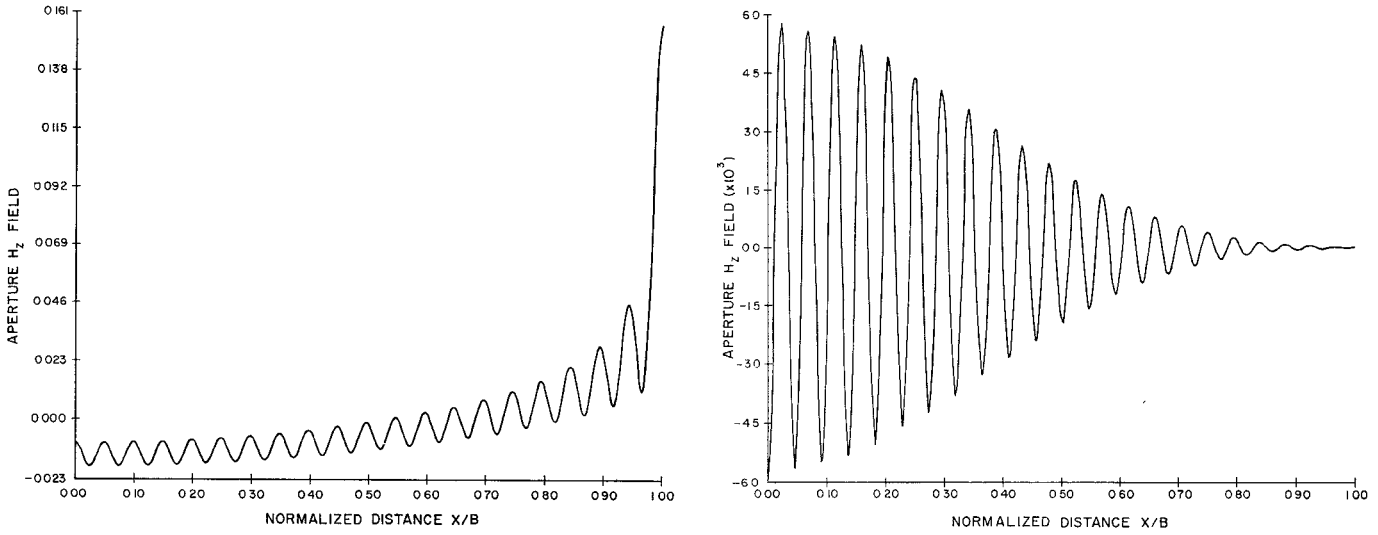

Fig. 9. Aperture H_z field for inductive iris. $b=0.4a$, $P=100$. (a) $M=40$. (b) $M=45$.

edge condition is indeed present in the numerically computed results for the H-field component transverse to the edges of the iris. To this end, the aperture H_z field was calculated and plotted in Fig. 9. The results clearly show that the H_z field becomes large as one approaches the edge of the iris. The figure also shows that following the pattern of the E_y field, the error in the computed H_z field also becomes large as M is increased beyond the critical value 40.

VI. Conclusions

An analytical explanation has been given for the relative convergence phenomenon arising in the solution of the integral equation for the iris discontinuity problem by the moment method. A numerical criterion for choosing the correct ratio of M/P has been suggested. The theoretical prediction has been verified by the numerical calculations.

For more general and complex structures, e.g., circular iris in rectangular waveguide, the simple analysis given here would not apply; hence, it would not be possible to derive an analytical criterion for the choice of the correct ratio of M/N. However, it appears[2] that for the general case, a numerical study of the higher order coefficients may be used as a reliable guide for choosing the critical ratio.

[2] This has in fact been successfully verified recently by solving the problem of a strip grating in a dielectric slab [13].

References

[1] R. Mittra, "Relative convergence of the solution of a doubly infinite set of equations," *J. Res. Nat. Bur. Stand.*, vol. 67D, Mar–Apr. 1963, pp. 245–254.
[2] D. S. Jones, *The Theory of Electromagnetism*. New York: Pergamon, 1964, pp. 566–569.
[3] A. Wexler, "Solution of waveguide discontinuities by modal analysis," *IEEE Trans. Microwave Theory Tech.*, vol. MTT-15, Sept. 1967, pp. 508–517.
[4] P. J. B. Clarricoats and C. D. Hannaford, "Computer method of solving waveguide-iris problems," *Electron. Lett.*, vol. 5, Jan. 23, 1969, pp. 23–25.
[5] S. W. Lee, W. R. Jones, and J. J. Campbell, "Convergence of numerical solution of iris-type discontinuity problems," *IEEE Trans. Microwave Theory Tech.*, vol. MTT-19, June 1971, pp. 528–536.
[6] P. J. B. Clarricoats and K. R. Slinn, "Numerical method for the solution of waveguide-discontinuity problems," *Electron. Lett.*, vol. 2, June 1966, pp. 226–228.
[7] P. R. Huckle and P. H. Masterman, "Analysis of a rectangular waveguide junction incorporating a row of rectangular posts," *Electron. Lett.*, vol. 5, Oct. 30, 1969, pp. 559–561.
[8] D. S. Jones, *The Theory of Electromagnetism*. New York: Pergamon, 1964, pp. 269–271.
[9] G. F. VanBlaricum, Jr., and R. Mittra, "Some analytical methods for solving a class of boundary value problems—Part I: Waveguide discontinuities," *IEEE Trans. Microwave Theory Tech.*, vol. MTT-17, June 1969, pp. 302–309.
——, "Some analytical methods for solving a class of boundary value problems—Part II: Waveguide phased arrays, modulated surfaces, and diffraction gratings," *ibid.*, pp. 310–319.
[10] R. Mittra and T. Itoh, "Charge and potential distributions in shielded striplines," *IEEE Trans. Microwave Theory Tech.*, vol. MTT-18, Mar. 1970, pp. 149–156.
[11] J. Mathews and R. L. Walker, *Mathematical Method of Physics*. New York: W. A. Benjamin, Inc., 1965, pp. 343–346.
[12] A. Erdelyi, *Tables of Integral Transforms*, vol. II (Bateman Project). New York: McGraw-Hill, 1954, pp. 215–262.
[13] T. Itoh and R. Mittra, "Relative convergence phenomenon arising in the solution of diffraction from strip grating on a dielectric slab," *Proc. IEEE* (Lett.), vol. 59, Sept. 1971, pp. 1363–1365.